

Cambridge Books Online

<http://ebooks.cambridge.org/>



Ideal MHD

Jeffrey P. Freidberg

Book DOI: <http://dx.doi.org/10.1017/CBO9780511795046>

Online ISBN: 9780511795046

Hardback ISBN: 9781107006256

Chapter

4 - MHD equilibrium: general considerations pp. 58-84

Chapter DOI: <http://dx.doi.org/10.1017/CBO9780511795046.005>

Cambridge University Press

4

MHD equilibrium: general considerations

4.1 Introduction

The goal of MHD equilibrium theory is the discovery of magnetic geometries that confine and isolate hot plasmas from material walls and are macroscopically stable at sufficiently high values of β (where β is plasma pressure/magnetic pressure) to be attractive as potential fusion reactors.

Research starting in the 1950s has led to the discovery of several magnetic geometries possessing such attractive MHD properties. Chapter 4 focuses on the general features common to these configurations. Included in the discussion are (1) a description of the basic equilibrium equations, (2) the need for toroidicity, (3) the concept of magnetic flux surfaces, (4) the definition of the basic plasma parameters and figures of merit describing an MHD equilibrium, and (5) the fundamental conflict between the requirements for good equilibrium and good stability in toroidal geometry. Thus, a framework and perspective are developed that provide an overview of the nature of MHD equilibria. This background, once established, is the basis for the discussions of the specific applications presented in the chapters that follow.

4.2 Basic equilibrium equations

To begin, consider the MHD equilibrium equations given by

$$\begin{aligned}\mathbf{J} \times \mathbf{B} &= \nabla p \\ \nabla \times \mathbf{B} &= \mu_0 \mathbf{J} \\ \nabla \cdot \mathbf{B} &= 0\end{aligned}\tag{4.1}$$

These are just the time-independent form of the full MHD equations with $\mathbf{v} = 0$; the equilibria of interest are static. Equilibrium is achieved by balancing the magnetic force $\mathbf{J} \times \mathbf{B}$ with the pressure gradient force ∇p .

It is worthwhile noting that while the full MHD equations including dynamics are valid for times comparable to the MHD time scale, the equilibrium equations themselves are actually valid over the much longer transport time scale. This follows because for static or very slowly moving systems, the issues of E_{\parallel} , collisions, and viscosity are either negligible or exactly cancel when adding the individual electron and ion momentum equations to obtain the single-fluid MHD momentum equation.

The question of static ($\mathbf{v} = 0$) vs. stationary ($\mathbf{v} \neq 0$) equilibria is also worth discussing. In many current fusion experiments substantial equilibrium flows are observed suggesting that stationary flows should be included in the analysis. Even so, such equilibrium flows are not included in the present textbook, primarily because of their mathematical complexity. Still, there is a wealth of information and insight that can be obtained by studying purely static MHD equilibria. This strategy thereby avoids the high level of complexity arising from the introduction of flow.

A final point of interest concerns the conservation of mass equation and the adiabatic equation of state. For static equilibria these relations are automatically satisfied. This implies that $\rho(\mathbf{r})$ is arbitrary and that $p(\mathbf{r})$ is decoupled from $\rho(\mathbf{r})$.

4.3 The virial theorem

The ideal MHD equilibrium equations satisfy a particular integral relation known as the virial theorem (Shafranov, 1966). A consequence of this theorem is the basic requirement that for an MHD equilibrium to exist, the plasma must be held in force balance by externally supplied currents; it is not possible to create a configuration confined solely by the currents flowing within the plasma itself. If this were possible, one could design a very attractive fusion reactor requiring only minimal “start-up” coils, which could be shut off once the plasma currents were established (see Fig. 4.1).

To demonstrate the virial theorem, recall that the equilibrium force balance equation can be written in conservation form,

$$\nabla \cdot \mathbf{T} = 0 \quad (4.2)$$

where the stress tensor \mathbf{T} is given by

$$\begin{aligned} \mathbf{T} &= p_{\perp}(\mathbf{I} - \mathbf{b}\mathbf{b}) + p_{\parallel}\mathbf{b}\mathbf{b} \\ p_{\perp} &= p + B^2/2\mu_0 \\ p_{\parallel} &= p - B^2/2\mu_0 \\ \mathbf{b} &= \mathbf{B}/B \end{aligned} \quad (4.3)$$

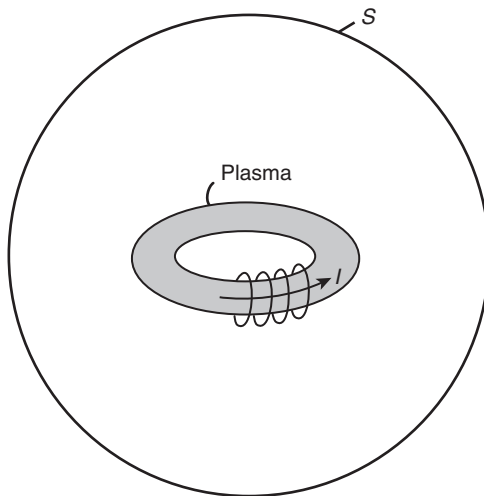


Figure 4.1 Geometry illustrating a plasma attempting to confine itself by its own currents. The surface S is the one referred to in the virial theorem.

Note that in a local orthogonal coordinate system with unit vectors $\mathbf{e}_1(\mathbf{r})$, $\mathbf{e}_2(\mathbf{r})$, $\mathbf{b}(\mathbf{r})$, \mathbf{T} has the form

$$\mathbf{T} = \begin{vmatrix} p_{\perp} & & \\ & p_{\perp} & \\ & & p_{\parallel} \end{vmatrix} \quad (4.4)$$

indicating that p_{\perp} and p_{\parallel} represent the stresses perpendicular and parallel to \mathbf{B} , respectively.

The next step in the derivation is to integrate the identity

$$\nabla \cdot (\mathbf{r} \cdot \mathbf{T}) = \mathbf{r} \cdot (\nabla \cdot \mathbf{T}) + \text{Trace}(\mathbf{T}) \quad (4.5)$$

over an arbitrary volume V , bounded by the surface S . Setting $\nabla \cdot \mathbf{T} = 0$ for equilibrium leads to

$$\int_V \left(3p + \frac{B^2}{2\mu_0} \right) d\mathbf{r} = \int_S \left[\left(p + \frac{B^2}{2\mu_0} \right) (\mathbf{n} \cdot \mathbf{r}) - \frac{B^2}{\mu_0} (\mathbf{r} \cdot \mathbf{b})(\mathbf{n} \cdot \mathbf{b}) \right] dS \quad (4.6)$$

where $d\mathbf{S} = \mathbf{n}dS$ and \mathbf{n} is the outward-pointing normal vector to S .

Assume now that the virial theorem is false; confined equilibria do exist without external currents. Let S lie outside the confined plasma so that $p(S) = 0$ (see Fig. 4.1). If no external currents are present, then S can extend to infinity. Furthermore, if as assumed, the equilibrium currents are indeed confined to the plasma, then B must decrease with radius for large r at least as rapidly as a dipole

field: $B(S) \leq K/r^3$ as $r \rightarrow \infty$. Consequently, for large r the integrand on the right-hand side of Eq. (4.6) scales as

$$\text{Integrand} \leq B^2 r dS \leq \frac{K^2 \sin \theta d\theta d\phi}{r^3} \quad (4.7)$$

Under these circumstances, as S extends to infinity, the right-hand side of Eq. (4.6) vanishes while the left-hand side approaches a non-zero positive constant. The resulting contradiction thus proves the virial theorem. When confined equilibria are surrounded by external conductors, Eq. (4.6) is not violated, since the right-hand side must now be evaluated over the surface of the conductors.

4.4 The need for toroidicity

The most obvious common feature of current magnetic fusion concepts is that, with one exception, each is constructed in the shape of a torus. The idea is to create configurations in which magnetic field lines remain contained within a closed toroidal volume; lines should not intersect the vacuum chamber.

The reason for building such technologically complicated toroidal systems rather than simpler, linear, open-ended systems is associated with the enormous difference in the energy loss rates perpendicular and parallel to the magnetic field. In an open-ended device, magnetic field lines leave the system and ultimately make contact with material walls (see Fig. 4.2a). Both particles and energy can be lost very quickly because charged particles move freely along magnetic field lines. Assuming that the potentially faster free streaming particle loss can be eliminated by magnetic trapping, the dominant parallel energy loss mechanism is due to collisional transport, in particular thermal conduction by electrons.

In contrast, for a toroidal device with contained magnetic lines (see Fig. 4.2b), cross field ion thermal conduction is the dominant loss mechanism. There are no

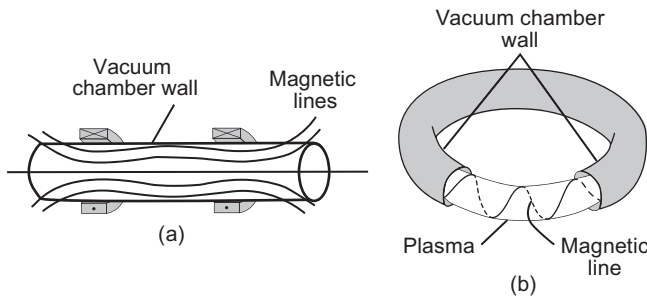


Figure 4.2 Magnetic field line trajectories in (a) an open-ended system and (b) a toroidal system.

parallel losses to the wall. The ratio of the parallel to perpendicular classical thermal conductivities is given by (Braginskii, 1965)

$$\frac{\kappa_{\parallel e}}{\kappa_{\perp i}} \approx \left(\frac{m_i}{m_e}\right)^{1/2} (\omega_{ci}\tau_i)^2 = 3.4 \times 10^{10} \left(\frac{B^2 T_k^3}{n_{20}^2}\right) \quad (4.8)$$

where ω_{ci} is the ion cyclotron frequency and τ_i is the characteristic ion–ion collision time for momentum exchange. It is also assumed that (1) the ions are singly charged deuterons, (2) the electrons and ions are at the same temperature, and (3) the Coulomb logarithm appearing in τ_i has been set to $\ln \Lambda = 19$. For plasma parameters corresponding either to current experimental operation or to reactor conditions this ratio is enormous. As an example, consider a tokamak with $T = 3$ keV, $B = 5$ T, and $n = 10^{20} \text{ m}^{-3}$. In this case $\kappa_{\parallel e}/\kappa_{\perp i} = 2.3 \times 10^{13}$!

In practice the actual value of the perpendicular thermal conductivity in a toroidal plasma is substantially larger than the classical value. The reasons for this are twofold. First, the orbits of a small class of trapped particles are strongly modified by toroidal effects, leading to a disproportionately large contribution to $\kappa_{\perp i}$ (neoclassical transport). Second, and more importantly, anomalous effects due to plasma micro-instabilities increase the effective collision frequency, leading to greatly enhanced values of $\kappa_{\perp i}$ and $\kappa_{\perp e}$. However, experimental measurements of $\kappa_{\parallel e}$ indicate that its value is approximately classical. Even with these larger values of $\kappa_{\perp i}$ the ratio of $\kappa_{\parallel e}/\kappa_{\perp i}$ remains so large that there exists a common consensus that, to avoid such losses, the magnetic configuration must be toroidal.

The one exception to this consensus is the open-ended mirror confinement concept. Here, by a combination of innovative ideas and clever plasma operation, large gains have been made in reducing end loss. However, even with these improvements in confinement, mirrors, as of this writing, have yet to achieve comparable performance to the tokamak. As a result the worldwide mirror program has been dramatically reduced in size with respect to its peak years in the 1970s and 1980s. A main focus of today's mirror program is based on the idea of the gas dynamic trap, whose goal is the development of a 14 MeV neutron source, a very important facility for testing materials in a fusion environment. The mirror machine may be attractive for this purpose because of reduced plasma confinement requirements and the possibility of a simple, very compact, low cost design.

4.5 Flux surfaces

In general, for a fusion plasma the magnetic field lines lie on a set of closed nested toroidal surfaces. This follows from the equilibrium relation obtained by forming the dot product of MHD momentum equation with \mathbf{B} :

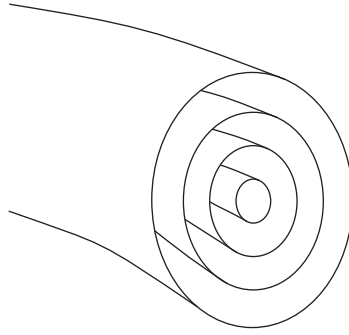


Figure 4.3 Contours of constant pressure in a well-confined toroidal equilibrium.

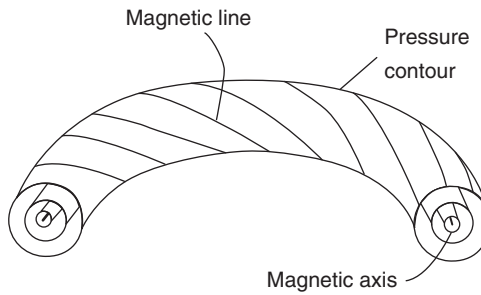


Figure 4.4 Toroidal flux surfaces showing the magnetic axis and the magnetic lines lying on a surface.

$$\mathbf{B} \cdot \nabla p = 0 \quad (4.9)$$

That is, for a well-confined equilibrium the pressure is maximum near the center of the poloidal cross section and is weakly varying around the toroidal direction. For such profiles the contours of constant pressure are nested toroidal surfaces (see Fig. 4.3). From Eq. (4.9) it follows that the magnetic lines lie on the $p = \text{constant}$ contours.

Consequently these contours are usually referred to as magnetic flux surfaces or simply just flux surfaces. The limiting flux surface, which approaches a single magnetic line where the pressure is a maximum, is called the magnetic axis (see Fig. 4.4).

A similar equilibrium relation is obtained by forming the dot product of the MHD momentum equation with \mathbf{J} ,

$$\mathbf{J} \cdot \nabla p = 0 \quad (4.10)$$

which implies that the current lines also lie on the surfaces of constant pressure; the current flows between and not across flux surfaces. Note that while both \mathbf{J} and \mathbf{B} lie

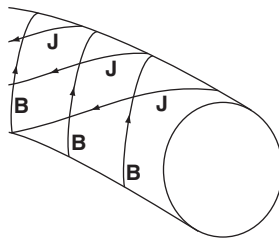


Figure 4.5 Toroidal flux surface showing magnetic lines and current lines lying on the surface. Note that the \mathbf{B} and \mathbf{J} lines are not in general purely parallel or perpendicular to each other.

on constant p contours, this does not imply that they are parallel. In general, the angle between \mathbf{J} and \mathbf{B} is arbitrary and the limits of being either purely parallel or perpendicular correspond to special cases. The general situation is illustrated in Fig. 4.5.

On any set of closed flux surfaces there are three important classes of magnetic field line trajectories that must be distinguished: rational, ergodic, and stochastic. A constant p contour on which all the lines exactly close on themselves after a finite number of toroidal circuits is known as a rational surface. If the field lines do not close, but instead wrap around indefinitely covering the entire constant p contour, this corresponds to an ergodic surface. Lastly, in those situations where the field line wanders around and actually fills a volume, the result is a region of stochasticity.

In general, toroidal magnetic geometries with ergodic or rational surfaces are the ones of interest and importance to fusion. Most configurations with desirable MHD confinement properties have both ergodic and rational surfaces. Usually the ratio of rational to ergodic surfaces is of measure zero. The tokamak, stellarator, reversed field pinch, and spheromak are configurations of this type. Concepts in which all field lines are rational on every flux surface are known as closed line systems. Two examples are the field reversed configuration and the levitated dipole.

Systems with regions of stochasticity are undesirable for fusion as they are characterized by poor confinement properties. Specifically, the equilibrium relation $\mathbf{B} \cdot \nabla p = 0$ implies that $p = \text{constant}$ over the stochastic volume, which is equivalent to a region with infinite transport. That is, the enormous parallel thermal conductivity of a plasma forces the temperature in the stochastic volume to rapidly equilibrate: $T = \text{constant}$ over the volume. Thus, to support a finite perpendicular heat flux $\mathbf{q}_\perp = -\kappa_\perp \nabla_\perp T$, assuming a flat temperature profile, one requires $\kappa_\perp \rightarrow \infty$. Stochastic regions can occur only in systems without geometric symmetry, for instance, in the vicinity of a separatrix in a 3-D stellarator or, more importantly, over substantial regions of plasma where there exists multidimensional

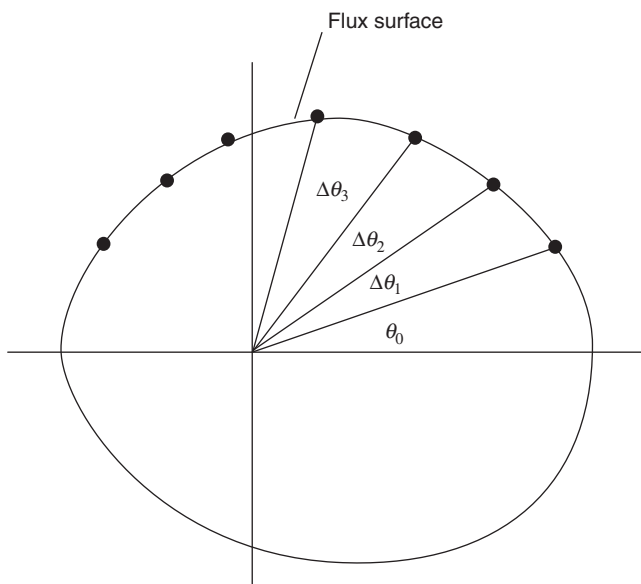


Figure 4.6 Magnetic field line projections used in the definition of rotational transform.

micro-turbulence involving a large number of different field harmonics. Because of their unattractive confinement properties, plasmas whose central core has regions of stochasticity should, to the maximal extent possible, be avoided experimentally. Consequently such systems are not treated here.

The usual way to characterize the two important classes of flux surfaces is in terms of the rotational transform, which is defined as follows. Imagine the projection of a magnetic line on a given poloidal cross section as shown in Fig. 4.6. The magnetic line starts off at a poloidal angle θ_0 . After one toroidal transit around the torus the magnetic line returns to a slightly different angle $\theta_0 + \Delta\theta$ on the flux surface. In general, $\Delta\theta$ depends upon the poloidal angle θ_0 , where the line started. The rotational transform ι is the average value of the angle $\Delta\theta$ after an infinite number of transits:

$$\iota = \lim_{N \rightarrow \infty} \frac{1}{N} \sum_{n=1}^N \Delta\theta_n \quad (4.11)$$

If ι is a rational fraction of 2π the line is closed. If it is not, the line is ergodic. The rotational transform plays an important role in both equilibrium and stability, and a practical procedure for its evaluation is discussed in Section 4.6. Note that ergodic surfaces can be mapped out either by plotting $p = \text{constant}$ contours or by tracing magnetic field line trajectories over many circuits of the torus. For closed line

systems, however, the flux surfaces are defined as $p = \text{constant}$ surfaces since closed lines do not trace out complete surfaces.

4.6 Surface quantities: basic plasma parameters and figures of merit

By carrying out appropriate integrals over the flux surfaces one can define a number of quantities that are of importance to the study of MHD equilibria. These quantities, known as “surface quantities,” describe the global properties of the equilibria. As such they are essential for distinguishing different configurations and for interpreting experimental data. Several quantities also serve as important figures of merit that provide insight into MHD stability. Furthermore, as discussed in the next section (Section 4.7), a precise number of freely chosen surface quantities must be specified a priori in order to formulate a well-posed equilibrium problem.

4.6.1 Fluxes and currents

Surface quantities are, in general, one-dimensional functions depending only upon the flux surface label. For example, each contour of the set of nested toroidal surfaces illustrated in Fig. 4.3 is labeled by a different value of the pressure p . If, as shown in Fig. 4.7, one now calculates the poloidal flux ψ_p contained within any given pressure contour

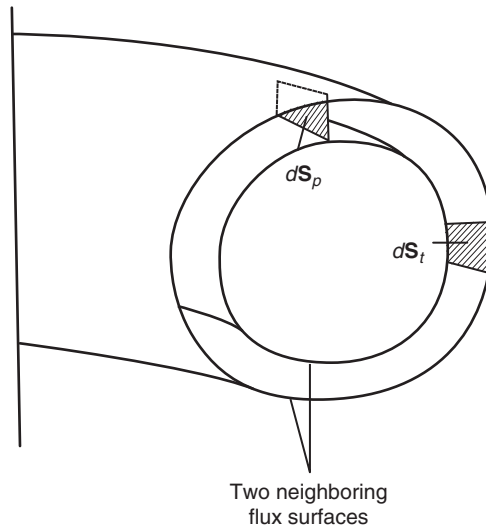


Figure 4.7 The poloidal and toroidal surface elements dS_p and dS_t used to calculate the corresponding magnetic fluxes.

$$\psi_p = \int \mathbf{B} \cdot d\mathbf{S}_p \quad \text{poloidal flux} \quad (4.12)$$

then

$$\psi_p = \psi_p(p) \quad (4.13)$$

The amount of poloidal flux contained within any given pressure contour depends only on the value of p labeling that contour.

Note that it makes physical sense for ψ_p to be a surface quantity since the magnetic lines lie in the constant p contours. Were the magnetic lines to cross the pressure surfaces, the definition of “contained flux” would become ambiguous. In fact, since \mathbf{J} and \mathbf{B} both lie on constant p contours, it follows that

$$\begin{aligned} \psi_t &= \int \mathbf{B} \cdot d\mathbf{S}_t && \text{toroidal flux} \\ I_t &= \int \mathbf{J} \cdot d\mathbf{S}_t && \text{toroidal current} \\ I_p &= \int \mathbf{J} \cdot d\mathbf{S}_p && \text{poloidal current} \end{aligned} \quad (4.14)$$

are also surface quantities. In contrast, the components of magnetic field and current density vary with the poloidal and toroidal angles, θ and ϕ , around a flux surface and thus do not qualify as surface quantities, i.e., on any surface $p = \text{constant}$, and B_p is a function $B_p(p, \theta, \phi)$ and not $B_p(p)$.

A further point concerns the labeling of the flux surfaces. Up until now it has been assumed that each flux surface has been labeled by a value of p . Clearly this is not unique. One could just as well label the surfaces with the values of ψ_p , or with any other surface quantity for that matter. In many MHD calculations appearing in the literature, either ψ_p , ψ_t , or a combination thereof is used as the label. The key point is that a properly defined surface quantity remains a surface quantity regardless of how the flux surfaces are labeled.

With this as background, one can now define several basic plasma parameters and figures of merit that measure the quality of an MHD equilibrium with respect to confinement efficiency and stability. All of the quantities introduced are discussed in detail in later sections of the textbook. For present purposes, they are simply introduced for convenience but with little accompanying discussion. Also, keep in mind that the figures of merit related to stability are in general neither necessary nor sufficient; instead, they serve as approximate guidelines for achieving overall favorable stability properties.

For a plasma parameter or figure of merit to be useful several requirements must be met: (1) the quantities must be relatively easy to evaluate but still accurately reflect the physics issue under consideration; (2) the quantities must be expressible

in terms of simple physical parameters, easily related to experiment; and (3) the quantities must be defined in a sufficiently general manner so as to apply to all configurations of interest.

The plasma parameters and figures of merit are now described below.

4.6.2 Normalized plasma pressure, β

The quantity β is a global plasma parameter whose value is critical for a fusion reactor. It measures the efficiency of plasma confinement by the magnetic field. Interestingly, there is actually no unique definition of plasma β that is agreed upon by the entire fusion community. Various definitions are distinguished by different geometric factors whose choice is motivated by a given configuration's aspect ratio and cross sectional shape. Still, there is usually not a large difference in numerical values between the various definitions. The definition used here and throughout the textbook follows the strategy of mathematical simplicity and ease of comparison with experiment.

Qualitatively, β measures the ratio of plasma pressure to magnetic pressure:

$$\beta = \frac{\text{plasma pressure}}{\text{magnetic pressure}} \quad (4.15)$$

The definition of plasma pressure is straightforward. It is assumed to be the volume averaged value defined as

$$\langle p \rangle = \frac{1}{V_p} \int p d\mathbf{r} \quad (4.16)$$

where V_p is the volume of the plasma.

It is the magnetic pressure, $B^2/2\mu_0$, that is more subtle. In general, both the toroidal and poloidal magnetic pressures must be included in the definition; that is, $B^2 = B_t^2 + B_p^2$. A convenient choice for the toroidal magnetic pressure for any cross section is $B_t^2 = B_0^2$, where B_0 is the vacuum toroidal field at the geometric center of the chamber confining the plasma: $R = R_0$ as shown in Fig. 4.8.

For the poloidal magnetic pressure a good choice for a circular cross section plasma is $B_p^2 = (\mu_0 I / 2\pi a)^2$ where I is the total toroidal plasma current and a is the minor radius of the plasma also shown in Fig. 4.8. This definition can be generalized to include non-circular plasmas as follows: $B_p^2 = (\mu_0 I / C_p)^2$. Here, C_p is the poloidal circumference of the plasma surface, which for simplicity is approximated by

$$C_p \approx 2\pi a \left(\frac{1 + \kappa^2}{2} \right)^{1/2} \quad (4.17)$$

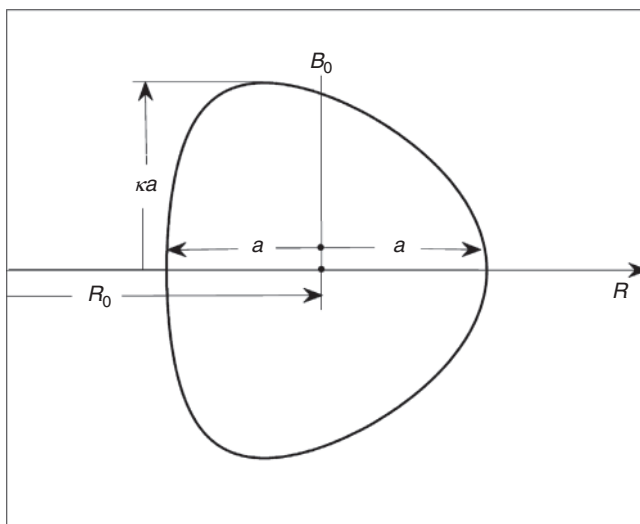


Figure 4.8 Geometry used in the evaluation of the figures of merit.

where κ is the plasma elongation as shown in Fig. 4.8. More accurate geometric approximations for the circumference can be made but they are more complicated mathematically and lead to only small quantitative changes in the value of C_p .

To summarize, the definition of β used throughout the textbook is given by

$$\beta = \frac{2\mu_0 \langle p \rangle}{B^2} \quad (4.18)$$

$$B^2 = B_0^2 + \left(\frac{\mu_0 I}{2\pi a} \right)^2 \frac{2}{1 + \kappa^2}$$

It is often useful to define separate toroidal and poloidal β s measuring plasma confinement efficiency with respect to each component of the magnetic field. These definitions have the form

$$\beta_t = \frac{2\mu_0 \langle p \rangle}{B_0^2} \quad (4.19)$$

$$\beta_p = \frac{4\pi^2 a^2 (1 + \kappa^2) \langle p \rangle}{\mu_0 I^2}$$

Note that

$$\frac{1}{\beta} = \frac{1}{\beta_t} + \frac{1}{\beta_p} \quad (4.20)$$

indicating that the smaller of the two quantities β_t or β_p dominates the overall magnetic confinement efficiency.

In general, high values of β are desirable for fusion reactor economics and technology. However, there is a maximum allowable value of β set by MHD equilibrium requirements and by MHD instabilities driven by the pressure gradient.

4.6.3 Kink safety factor, q_*

The kink safety factor is a global plasma parameter that measures stability against dangerous long-wavelength modes driven by the toroidal plasma current. These are known as “kink modes.” The kink safety factor is proportional to the ratio of toroidal field to toroidal current. High values provide “safety” against current-driven modes. The kink safety factor for a circular cross section plasma is defined by

$$q_* = \frac{aB_t}{R_0B_p} = \frac{2\pi a^2 B_0}{\mu_0 R_0 I} \quad (4.21)$$

The definition is extended to include non-circular cross sections by replacing $a \rightarrow C_p/2\pi \approx a[(1 + \kappa^2)/2]^{1/2}$. Thus, the definition used throughout the text is given by

$$q_* = \frac{2\pi a^2 B_0}{\mu_0 R_0 I} \left(\frac{1 + \kappa^2}{2} \right) \quad (4.22)$$

Observe that with this definition of q_* there is a simple relationship between β_t and β_p which can be written as

$$\frac{\beta_t q_*^2}{\varepsilon} = \varepsilon \beta_p \left(\frac{1 + \kappa^2}{2} \right) \quad (4.23)$$

In many fusion applications it is desirable to operate at high current (i.e., low q_*), for improved confinement and ohmic heating. However, kink instabilities prevent this type of operation and set a lower limit on the minimum achievable q_* (i.e., the maximum toroidal current).

4.6.4 Rotational transform, ι , and the MHD safety factor, q

The concept of the rotational transform ι has already been discussed in Section 4.5. Recall that the rotational transform is a surface quantity whose profile plays an important role in the MHD equilibrium and stability of magnetic fusion concepts. Its magnitude and profile have important consequences for the

maximum achievable β in a reactor. Usually the quantity $\iota/2\pi$ is directly used to describe 3-D configurations such as the stellarator. However, the inverse of $\iota/2\pi$, known as the safety factor q (not to be confused with the kink safety factor q_*), is the quantity that is typically used to describe 2-D axisymmetric configurations such as the tokamak and reversed field pinch. The relation between q and ι is thus given by

$$q = \frac{2\pi}{\iota} \quad (4.24)$$

As its name implies the “safety factor” is a qualitative indicator of stability. High q is “good” for stability while low q is “bad.”

Below a practical method is described for calculating the rotational transform in a multidimensional geometry. The starting assumptions are that a set of nested toroidal ergodic flux surfaces exist and that an MHD equilibrium has been calculated. Specifically, it is assumed that the magnetic fields $B_r(r, \theta, \phi)$, $B_\theta(r, \theta, \phi)$, and $B_\phi(r, \theta, \phi)$ are known quantities. Using this information one can calculate the field line trajectories $r(l)$, $\theta(l)$, and $\phi(l)$, where l is the arc length coordinate along the magnetic field. The trajectories are obtained by solving the following set of non-linear, first-order differential equations describing the tangent lines to the magnetic field:

$$\begin{aligned} \frac{dr}{dl} &= \frac{B_r}{B} \\ \frac{d\theta}{dl} &= \frac{B_\theta}{rB} \\ \frac{d\phi}{dl} &= \frac{B_\phi}{RB} \end{aligned} \quad (4.25)$$

where $R = R_0 + r \cos \theta$. For initial conditions at $l = 0$ assume that $\theta(0) = 0$, $\phi(0) = 0$, and $r(0) = r_0$. In this case the quantity r_0 serves as the flux surface label. Solving these equations is a straightforward numerical task.

Assume now that the field line trajectories are known. Then, over a segment of field line of length L , the changes in poloidal angle $\Delta\theta$ and toroidal angle $\Delta\phi$ are given by

$$\begin{aligned} \Delta\theta &= \int_0^{\Delta\theta} d\theta = \int_0^L \frac{d\theta}{dl} dl = \int_0^L \frac{B_\theta}{rB} dl \\ \Delta\phi &= \int_0^{\Delta\phi} d\phi = \int_0^L \frac{d\phi}{dl} dl = \int_0^L \frac{B_\phi}{RB} dl \end{aligned} \quad (4.26)$$

One now takes the limit $L \rightarrow \infty$. The rotational transform is just the average value of the poloidal excursion per single toroidal transit. Simple proportions then yield

$$\frac{\lim_{L \rightarrow \infty} \Delta\theta}{\lim_{L \rightarrow \infty} \Delta\phi} = \frac{i}{2\pi} \quad (4.27)$$

Equation (4.27) can conveniently be rewritten in terms of the safety factor

$$q = \frac{\lim_{L \rightarrow \infty} \int_0^L \frac{B_\phi}{RB} dl}{\lim_{L \rightarrow \infty} \int_0^L \frac{B_\theta}{rB} dl} \quad (4.28)$$

where the integrands $I_\phi = B_\phi/RB$ and $I_\theta = B_\theta/rB$ are evaluated along the field line trajectory. For example, $I_\phi(r, \theta, \phi) = I_\phi[r(l, r_0), \theta(l, r_0), \phi(l, r_0)] = I_\phi(l, r_0)$.

Equation (4.28) is the desired result. It defines the surface quantity $q(r_0)$ whose profile is important to know for all fusion concepts of interest. Simplified forms of $q(r_0)$ are derived in Chapters 5, 6, and 7 for 1-D, 2-D, and 3-D configurations. Qualitatively, a $q(r_0)$ profile that has a strong radial variation is said to possess magnetic shear, defined as $s(r_0) = (r_0/q)(dq/dr_0)$. In general, large shear is favorable for MHD stability.

Finally, it is worth noting that in certain special limits it just so happens that $q(\text{plasma edge}) = q_*$, a result that sometimes leads to confusion as to the role each plays. These difficulties are resolved in the discussion on tokamak stability.

4.6.5 Summary

A number of basic plasma parameters and figures of merit have been introduced whose purpose is to provide intuition as to the quality and desirability of a given MHD equilibrium for fusion applications. Of particular interest to the equilibrium confinement properties are the values of β and q_* as well as the profile of $i/2\pi$ or, equivalently q . In terms of stability attractive fusion concepts have a high maximum β , low minimum q_* , and a q profile with substantial shear.

4.7 Equilibrium degrees of freedom

In addition to their importance in describing the global properties of fusion plasmas, the surface quantities play a crucial role in the proper formulation of an MHD equilibrium problem. The reason is that while many different surface quantities can be defined, only two are independent. This can be seen intuitively by recognizing that there are two independent external circuits that control the properties of any given MHD equilibrium: one is the toroidal field circuit (e.g.,

regulate the toroidal flux evolution) and the other is the poloidal field circuit (e.g., regulate the toroidal current evolution). The existence of two arbitrary free surface functions has been demonstrated mathematically for one-, two- and general three-dimensional configurations.

The implication is that in order to formulate a well-posed MHD equilibrium problem it must be both possible and necessary to specify a priori two and only two independent surface quantities.

The existence of two free functions is on the one hand a great advantage of MHD equilibrium theory. This freedom allows the theory to describe a wide range of configurations. On the other hand, one must appreciate that the physics content of the ideal MHD model is insufficient to predict the specific functional dependence of the two free functions. Hence, for a given configuration the accuracy of the results depends upon the accuracy with which the free functions can be specified. For example, if $p(S)$ and $q(S)$ are chosen as the free functions, their dependence must be specified at the outset of the problem, based on physical intuition, experimental data, or the results of a transport code. Only after these functions are specified is the MHD equilibrium problem properly formulated, permitting a solution for the fields, flux surfaces, etc.

4.8 The basic problem of toroidal equilibrium

Qualitatively, the problem of producing a magnetically confined toroidal equilibrium separates into two parts. First, the magnetic configuration must provide radial pressure balance in the poloidal plane so that the pressure contours form closed nested surfaces (see Fig. 4.9). Both toroidal and poloidal fields can readily

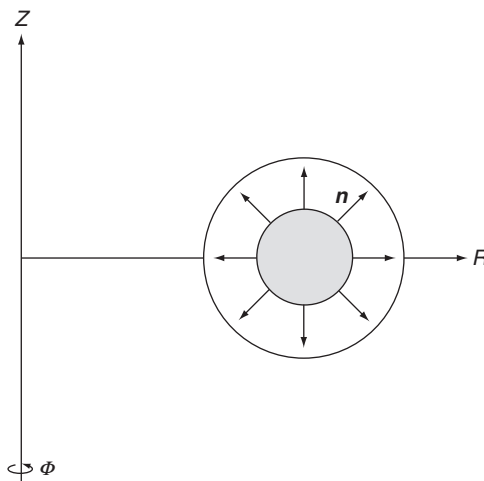


Figure 4.9 Schematic diagram of the forces required for radial pressure balance.

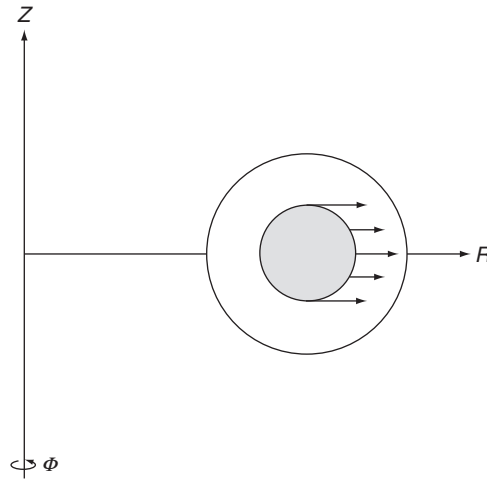


Figure 4.10 Schematic diagram of the outward toroidal expansion force inherent in all toroidal configurations.

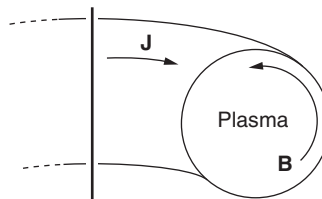


Figure 4.11 Toroidal configuration with a purely poloidal magnetic field.

accomplish this task although the manners in which they do so are quite different. Second, the configuration must balance the radially outward expansion force inherent in all toroidal geometries without sacrificing stability. This is known as toroidal force balance and is illustrated in Fig. 4.10. Although the forces associated with toroidal force balance are usually smaller than those corresponding to radial pressure balance, they are nevertheless more difficult to compensate. With this in mind it is helpful to examine two opposing limits that serve to illustrate the basic nature of the toroidal force balance problem.

To begin, consider a configuration with a purely poloidal magnetic field as shown in Fig. 4.11. There are two forces that cause the plasma to expand radially outward in the positive R direction: (1) the hoop force and (2) the tire tube force.

The hoop force arises because of toroidal current flowing in the plasma and is similar to the force produced by a current-carrying loop of wire. One can understand this force intuitively by examining the field pattern illustrated in Fig. 4.12a. Conservation of flux implies that $\psi_1 = \psi_2$. Since ψ_1 passes through a smaller area

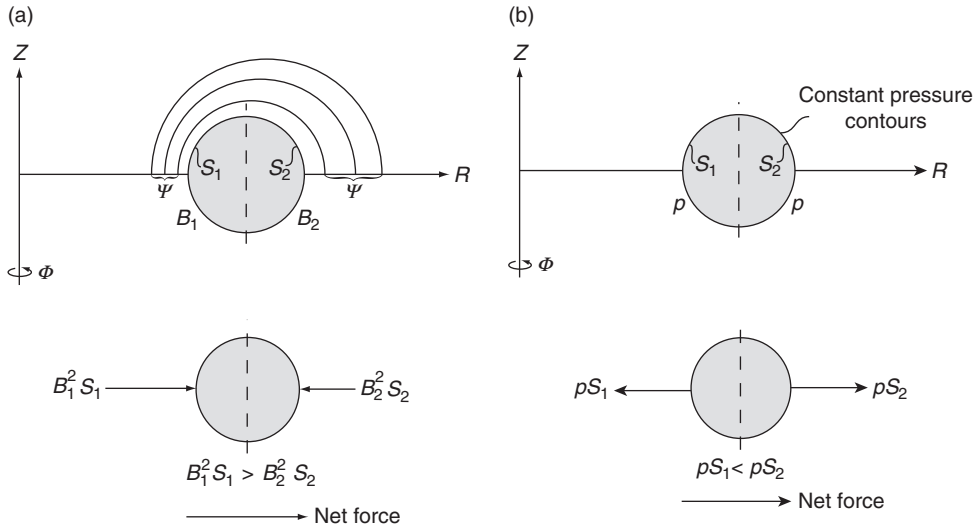


Figure 4.12 The toroidal expansion forces in a system with purely poloidal fields: (a) the hoop force and (b) the tire tube force.

than ψ_2 , one expects the average magnetic field on the inner plasma surface S_1 to be greater than that on the outer surface S_2 : $B_1 > B_2$. The net outward force on the plasma along R is proportional to $\mathbf{F}_R \propto \mathbf{e}_R(B_1^2 S_1 - B_2^2 S_2)/2\mu_0$. Even though S_1 is smaller than S_2 the quadratic dependence on B dominates, indicating that $\mathbf{F}_R > 0$: \mathbf{F}_R represents the outward hoop force.

The tire tube force arises as follows. On a constant pressure contour the area S_1 on the inside of the surface is smaller than the area S_2 on the outside: $S_1 < S_2$ (see Fig. 4.12b). If the pressure on this contour is denoted by p then there is a net outward force along R proportional to $\mathbf{F}_R \propto -\mathbf{e}_R(p S_1 - p S_2)$. Since $S_1 < S_2$ then $\mathbf{F}_R > 0$: \mathbf{F}_R represents an outward force very similar to that found in a rubber tire tube.

The combined outward force can be balanced in two different ways. First, if a perfectly conducting shell surrounds the plasma, then as the plasma expands along R in response to the outward force the poloidal magnetic flux outside the plasma is compressed, thereby increasing the magnetic pressure (Fig. 4.13a). Equilibrium is achieved when the plasma shifts sufficiently far out so that the increased magnetic pressure is large enough to balance the hoop plus tire tube forces.

A second way to balance the outward force is to replace the conducting wall with a set of fixed current-carrying vertical field coils (Fig. 4.13b). This is an important practical option. In actual experiments with conducting walls the materials used are usually copper, aluminum, or stainless steel, which have a high but not infinite conductivity. Hence, flux can only remain compressed for about a skin

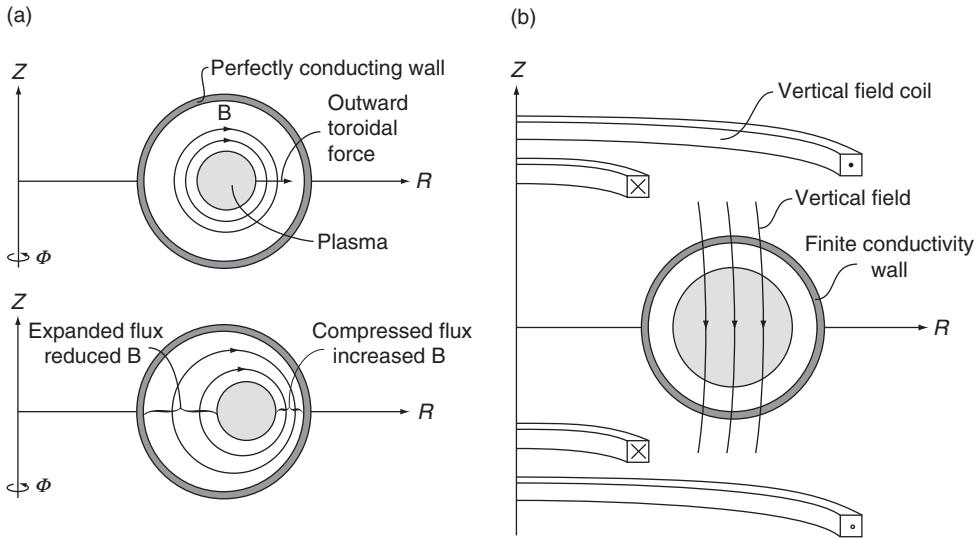


Figure 4.13 A configuration with purely poloidal fields held in toroidal equilibrium by means of (a) a perfectly conducting wall and (b) an externally applied vertical field.

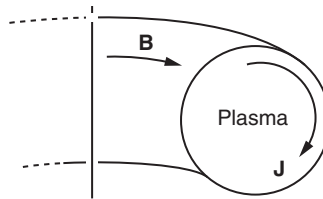


Figure 4.14 Toroidal configuration with a purely toroidal field.

time, which is with rare exceptions shorter than the experimental times of interest. By a proper choice of magnitude and sign, the vertical field generated by the external coils produces an inward compensating $\mathbf{J} \times \mathbf{B}_{\text{vert}}$ force for equilibrium: $\mathbf{F}_R = \mathbf{e}_R 2\pi R_0 I B_{\text{vert}}$. Thus, configurations with purely poloidal magnetic fields can be readily designed with good toroidal equilibrium properties.

This favorable equilibrium conclusion is negated by the fact that such configurations often develop catastrophic MHD instabilities leading to the destruction of the plasma. (The stability of configurations with purely poloidal fields is discussed in detail in Chapter 11.)

As a consequence, one is motivated to examine the opposite limit, a configuration with a purely toroidal field as shown in Fig. 4.14. In Chapter 11, it is demonstrated that this configuration has inherently better stability properties than

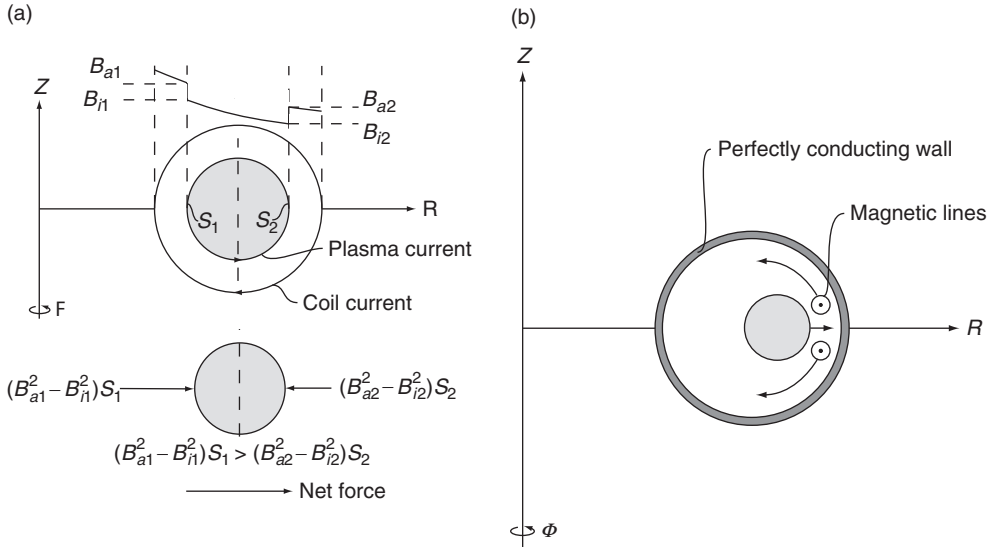


Figure 4.15 Toroidal force balance in a configuration with a purely toroidal field: (a) sharp boundary model showing the $1/R$ outward force and (b) the lack of toroidal equilibrium.

that corresponding to a purely poloidal field. Nevertheless, from the simple calculation outlined below, it follows that a purely toroidal configuration cannot be held in MHD equilibrium.

To show this, assume for simplicity that the plasma carries only a diamagnetic surface current: $B_{a1} > B_{i1}$ and $B_{a2} > B_{i2}$ (see Fig. 4.15b). The implication is that some toroidal field is excluded from the plasma interior. From Maxwell's equations it follows that the toroidal field in both the plasma and vacuum decrease inversely with R ; that is $\mathbf{B} = B_\phi \mathbf{e}_\phi$ where

$$\begin{aligned}\hat{B}_\phi &= \hat{K}/R \\ B_\phi &= K/R\end{aligned}\tag{4.29}$$

and $\hat{K} > K$.

Because of the $1/R$ dependence it is clear that the magnetic field on the inside of the torus is always greater than that on the outside: $B_1 > B_2$. This effect is partially compensated by the slightly smaller area on the inside $S_1 < S_2$, but the quadratic dependence of the magnetic pressure on B dominates and there remains a net outward force: $\mathbf{F}_R \propto \mathbf{e}_R [(B_{a1}^2 - B_{i1}^2)S_1 - (B_{a2}^2 - B_{i2}^2)S_2]/2\mu_0$. There is an additional outward force arising from the tire tube effect, identical to that in the purely poloidal case.

The end result is that a diamagnetic plasma confined solely by a toroidal field also experiences a radially outward toroidal expansion force. One can now ask whether or not this force can be balanced in a similar manner to the purely poloidal case. The answer is no! The explanation is as follows.

Since the magnetic field is in the toroidal direction, a conducting wall is not able to compensate the outward force; that is, as the plasma moves outward the magnetic lines simply slip around and let the plasma drift through (Fig. 4.16b); because of the topology, toroidal flux does not get trapped between the plasma and the wall. Likewise, a vertical field does not help because by symmetry the $\mathbf{J} \times \mathbf{B}_{\text{vert}}$ force does not point along R .

The conclusion from this discussion is that a configuration with a purely toroidal magnetic field cannot be held in MHD equilibrium because of the $1/R$ dependence of B_ϕ resulting from the toroidal geometry.

The basic problem of finding attractive magnetic geometries for confining fusion plasmas can thus be summarized as follows. On the one hand, toroidal systems with a purely poloidal magnetic field have good toroidal equilibrium properties but poor stability properties. On the other hand, for a pure toroidal field, stability is inherently much better, but serious equilibrium problems exist. Attempts to resolve this dilemma have led to the discovery of a number of different configurations whose strategy is to combine the desirable features of both toroidal and poloidal systems while to a reasonable extent suppressing the undesirable ones. Chapters 5–7 discuss the equilibrium properties of the currently most promising magnetic configurations.

4.9 A single particle picture of toroidal equilibrium

The final topic in this chapter is aimed at developing further intuition into the basic problem of toroidal equilibrium by re-examining the issues from the point of view of single particle guiding center motion.

Consider first the equilibrium problem in the case of a purely toroidal field. For a low β plasma with small diamagnetism the dominant drifts experienced by the particles are due to ∇B and curvature. These drifts arise because of the $1/R$ dependence of B and the centrifugal force, both toroidal effects. As illustrated in Fig. 4.16 the guiding center drift velocity is in the Z direction and is given by

$$\mathbf{V}_{g\perp} = \frac{1}{\omega_{c0}R_0} \left(\frac{w_\perp^2}{2} + w_\parallel^2 \right) \mathbf{e}_Z \quad (4.30)$$

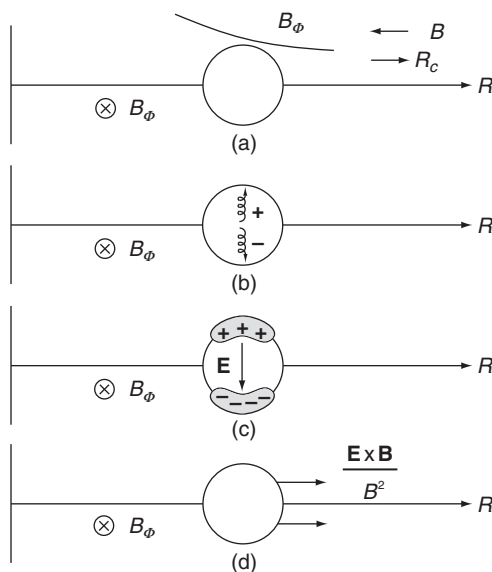


Figure 4.16 Single particle picture illustrating the lack of toroidal equilibrium in a system with purely toroidal field: (a) the geometry, (b) the guiding center drifts, (c) the induced electric field, and (d) the induced outward $\mathbf{E} \times \mathbf{B}$ drift.

where $\omega_{c0} = qB_0/m$. Note that the drift is in opposite directions for electrons and ions. As a result, positive and negative charges collect at the top and bottom of the plasma, respectively, as shown in Fig. 4.16. This charge sets up a Z directed electric field, which then propels the entire plasma outward along R with the $(\mathbf{E} \times \mathbf{B})/B^2$ drift velocity. Hence, there is no toroidal equilibrium for a configuration with purely toroidal field.

What happens when a poloidal field is superimposed on the toroidal field? In this case the magnetic field lines wrap around the plasma on helical trajectories similar to the stripes on a barber pole. Even so, the particles still experience the same up–down drift given by Eq. (4.30). One is now faced with the apparently paradoxical question of how the addition of a poloidal field can lead to single particle confinement for particles that are always drifting upward (or downward for the opposite charge).

The resolution is illustrated in Fig. 4.17. Here, the dashed lines represent flux surfaces. To leading order, the parallel motion of a particle simply follows a field line. Thus, the projection of the particle's guiding center orbit onto a poloidal cross section would exactly coincide with the flux surface if there was no vertical drift. However, when the drift is included, then as the particle spirals along the field line from point 1, it actually arrives at point 2, off the original surface, because of the

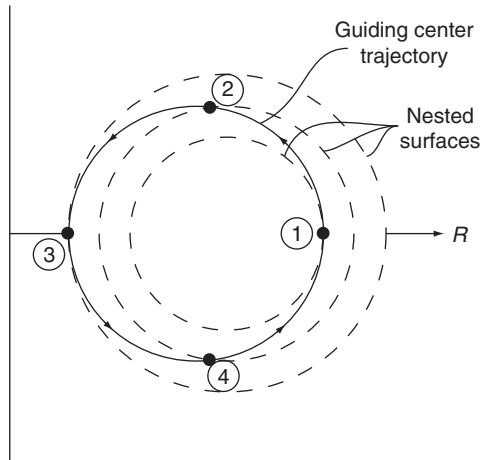


Figure 4.17 Single particle picture of toroidal confinement due to the presence of a poloidal magnetic field. Shown is a particle orbit including a uniform upward drift.

upward drift. From point 2 to 3 the drift off the surface continues to increase. In contrast, from point 3 to 4 and then back to 1, the upward drift actually causes the particle to drift back toward the surface, eventually returning to its starting position.

The point is that a constant upward drift corresponds to motion away from the surface half the time and toward the surface the other half of the time; on average the net motion due to the drift cancels and the particles remain confined. This simple picture demonstrates how a poloidal field leads to single particle confinement and macroscopic toroidal force balance.

4.10 Summary

Ideal MHD equilibrium theory has the goal of discovering magnetic geometries that stably confine hot plasmas at sufficiently high values of β to be of interest as fusion reactors. Over years of research many different concepts have been developed to achieve this goal. These different concepts, nevertheless, share a number of common features, which have been the subject of Chapter 4. A summary is given below.

- **Basic equations:** The equilibrium equations of interest correspond to the time-independent $\partial/\partial t = 0$, static $\mathbf{v} = 0$, limit of the MHD model, which describes a balance between the pressure gradient force ∇p and the magnetic

force $\mathbf{J} \times \mathbf{B}$. The equilibrium model by itself is actually valid from the MHD time scale up until the very long transport time scale.

- **Virial theorem:** The virial theorem demonstrates that as desirable as it may be, it is not possible to construct a magnetic geometry in which the plasma is confined solely by its own currents; an external coil system must be supplied.
- **Toroidicity:** Because the thermal conduction loss rate parallel to the magnetic field is enormous compared to that perpendicular to the field, there is near consensus in the fusion community that magnetic geometries of fusion interest must be toroidal. The one important exception to this philosophy is the mirror concept.
- **Magnetic flux surfaces:** In a well-confined toroidal MHD equilibrium, the contours of constant pressure form a set of nested tori. Both the magnetic and current lines lie on these contours, which are known as flux surfaces.
- **Surface quantities and figures of merit:** For any given MHD equilibrium, it is possible to define a number of global quantities that depending only upon the flux surface label. These surface quantities represent important physical parameters which can be related to experiment and be used as figures of merit for measuring stability. Included are average beta β , toroidal beta β_t , poloidal beta β_p , kink safety factor q_* , rotational transform $i/2\pi$, and MHD safety factor q .
- **Equilibrium degrees of freedom:** For a well-posed MHD equilibrium problem it must be both possible and necessary to specify a priori two and only two independent surface quantities.
- **The basic problem of toroidal equilibrium:** The problem of MHD equilibrium separates into two parts: radial pressure balance and toroidal force balance. The latter is the more difficult problem and herein lies the basic dilemma of magnetic fusion geometries. Systems with a purely poloidal magnetic field are easy to maintain in toroidal force balance but have poor MHD stability properties. In contrast, systems with a purely toroidal field have poor toroidal force balance but much more favorable stability properties (in equivalent straight systems). The challenge then is to discover configurations which combine the favorable features and minimize the unfavorable features of these two limiting configurations.

References

- Braginskii, S. I. (1965). In *Reviews of Plasma Physics*, Vol. 1, ed. M. A. Leontovich. New York: Consultants Bureau.
- Shafranov, V. D. (1966). In *Reviews of Plasma Physics*, Vol. 2, ed. M. A. Leontovich. New York: Consultants Bureau.

Further reading

The references below all have detailed discussions concerning the basic properties of MHD equilibrium.

Bateman, G. (1978). *MHD Instabilities*. Cambridge, MA: MIT Press.

Bellan, P. M. (2006). *Fundamentals of Plasma Physics*. Cambridge: Cambridge University Press.

Goedbloed, J. P. and Poedts, S. (2004). *Principles of Magnetohydrodynamics*. Cambridge: Cambridge University Press.

Hazeltine, R. D. and Meiss, J. D. (2003). *Plasma Confinement*. Redwood City, CA: Addison-Wesley.

Morozov, A. I. and Solov'ev, L. S. (1966). In *Reviews of Plasma Physics*, Vol. 2, ed. M. A. Leontovich. New York: Consultants Bureau.

Shafranov, V. D. (1966). In *Reviews of Plasma Physics*, Vol. 2, ed. M. A. Leontovich. New York: Consultants Bureau.

Solov'ev, L. S. and Shafranov, V. D. (1970). In *Review of Plasma Physics*, Vol. 5, ed. M. A. Leontovich. New York: Consultants Bureau.

Wesson, J. (2011). *Tokamaks*, 4th edn. Oxford: Oxford University Press.

Problems

4.1 For each of the magnetic configurations given below calculate B_r and then determine the magnetic field line trajectories and the shape of the flux surfaces.

(a) $B_\theta = B_{\theta 0}[ar/(r^2 + a^2)]$
 $B_z = B_{z0}$
 with $B_{\theta 0}$, B_{z0} , and a constants

(b) $B_\theta = 0$
 $B_z = B_{z0}(1 + \delta \cos kz)$
 with B_{z0} and δ constants

(c) $B_\theta = B_{\theta 0}(r + \Delta \cos \theta)/a$
 $B_z = B_{z0}$
 with $B_{\theta 0}$, B_{z0} , a , and Δ constants

4.2 Following the discussion associated with Fig. 4.17 sketch the orbit of a particle starting off at point 1 with a parallel velocity in the opposite direction of that illustrated.

4.3 Show that the MHD equilibrium equations for an arbitrary three-dimensional geometry can be written as

$$\nabla_\perp \left(p + \frac{B^2}{2\mu_0} \right) - \frac{B^2}{\mu_0} \boldsymbol{\kappa} = 0$$

where $\boldsymbol{\kappa} = \mathbf{b} \cdot \nabla \mathbf{b}$ is the field line curvature and $\mathbf{b} = \mathbf{B}/B$.

4.4 The goal of this problem is to calculate the volume contained within a given flux surface. The starting point is the usual definition of volume given by

$$V = \int d\mathbf{r} = \int_0^{2\pi} d\phi \int_0^{2\pi} d\theta \int_0^{r_s} R r dr$$

Here $R = R_0 + r_s \cos \theta$, $r_s = r_s(\theta, \phi, r_0)$ specifies the shape of the flux surface and r_0 is the label for the flux surface under consideration. See Fig. 4.8 for the geometry. Note that an alternate representation of the flux surface can be written as $S(r_s, \theta, \phi) = S_0$ where S_0 now represents the flux surface label.

- (a) Make a change of variables from r, θ, ϕ to S, θ, ϕ and show that the volume of an arbitrary 3-D flux surface can be written as

$$V = \int_0^{S_0} dS \int_0^{2\pi} \int_0^{2\pi} \frac{R r_s}{\partial S / \partial r_s} d\theta d\phi$$

- (b) For a 1-D system with cylindrical symmetry set $S = r$ and $S_0 = r_0$. Show that the volume, as expected, is given by $V(r_0) = 2\pi^2 R_0 r_0^2$.
- (c) Consider now a 2-D system with toroidal symmetry: $\partial/\partial\phi = 0$. In this case any divergence free poloidal magnetic field can be written as $\mathbf{B}_p = \nabla\psi \times \nabla\phi$ where $\psi = \psi(S)$ is an appropriately scaled flux surface label. Show that the expression for the volume reduces to

$$V(\psi_0) = 2\pi \int_0^{\psi_0} d\psi \oint \frac{dl_p}{B_p}$$

4.5 This problem investigates the approximation $C_p \approx 2\pi a[(1 + \kappa^2)/2]^{1/2}$ used in the definition of q_* . For the following model cross sections calculate and plot $C_p/2\pi a$ as a function of elongation κ over the range $1 \leq \kappa \leq 3$. The geometry for each cross section is shown in Fig. 4.18.

- (a) An ellipse (this involves elliptic functions).
- (b) A racetrack.
- (c) A triangle plasma.
- (d) A “D” shaped plasma.
- (e) The approximation $C_p/2\pi a \approx [(1 + \kappa^2)/2]^{1/2}$.

How big are the errors between the approximation and the exact values for the various cross sections?

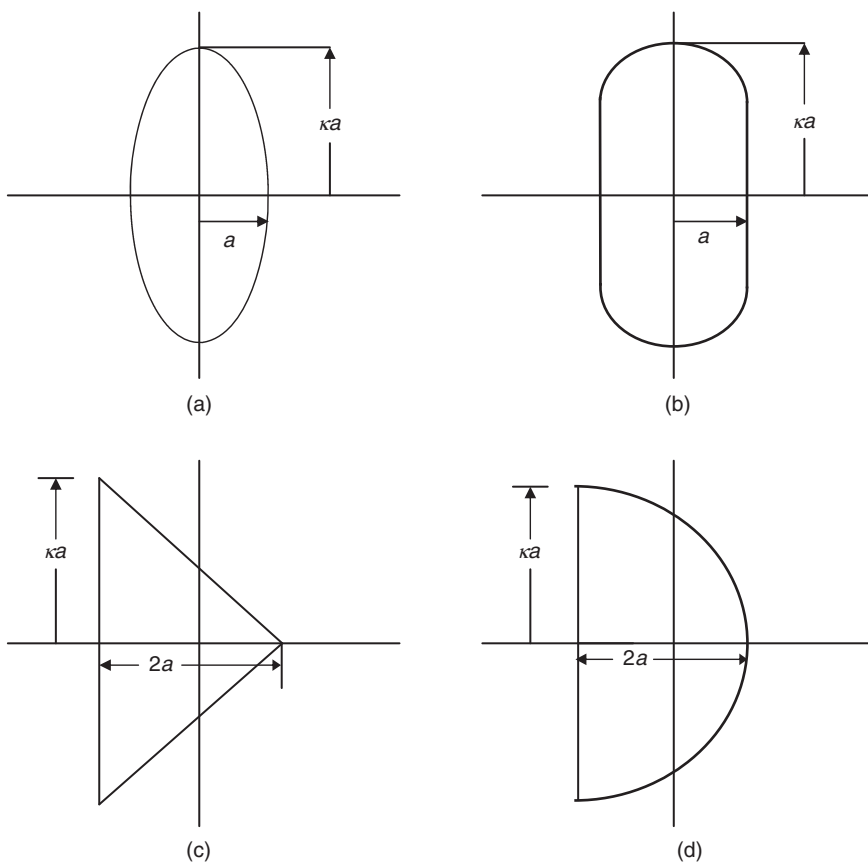


Figure 4.18 Geometry for various cross sections: (a) ellipse, (b) racetrack, (c) triangle plasma, and (d) "D" shaped plasma